scientific reports

Check for updates

OPEN

Maid gene dysfunction promotes hyperobesity via the reduction of adipose tissue inflammation in Mc4r gene-deficient mice

Kyutaro Koyama[1], Akira Sakamaki[1]✉, Shinichi Morita[1], Itsuo Nagayama[1], Marina Kudo[1], Yuto Tanaka[1], Naruhiro Kimura[1], Yoshihisa Arao[1], Hiroyuki Abe[1], Kenya Kamimura[2] & Shuji Terai[1]✉

The onset and progression mechanisms of metabolic dysfunction-associated steatotic liver disease (MASLD) and metabolic dysfunction-associated steatohepatitis (MASH) are being studied. We developed and analyzed a new mouse model of obesity by combining maternal Id-like molecule (Maid) and melanocortin-4 receptor (Mc4r) gene deletions. Four mice, each at 12 and 28 weeks of age, were analyzed for each genotype: Maid gene knockout, Mc4r gene knockout, combined Mc4r and Maid gene knockout, and Mc4r gene knockout with a high-fat diet. Mice with a combined deficiency of Mc4r and Maid gene showed significantly more severe obesity compared to all other genotypes, but no liver fibrosis or a decline in metabolic status were observed. In visceral white adipose tissue, Maid and Mc4r gene knockout mice had fewer CD11c-positive cells and lower mRNA expression of both inflammatory and anti-inflammatory cytokines. Furthermore, Maid and Mc4r gene knockout mice showed lower expression of adipocytokines in visceral white adipose tissue and uncoupling protein-1 in scapular brown adipose tissue. The expression of adipocytokines and uncoupling protein-1 is regulated by sympathetic nerve signaling that contribute severe obesity in Maid and Mc4r gene knockout mice. These mechanisms contribute hyperobesity in Maid and Mc4r gene knockout mice.

As a result of significant advances in medication for viral hepatitis, cirrhosis[1] and hepatocellular carcinoma[2] caused by viral hepatitis have decreased. However, there is an increasing the number of patients with nonalcoholic fatty liver disease (NAFLD) and nonalcoholic steatohepatitis (NASH)[3,4]. Although the development rate of liver fibrosis and cirrhosis from NAFLD is lower than that of viral hepatitis, the actual number of patients with cirrhosis caused by NAFLD is high due to its prevalence[4]. Several mechanisms have been reported underlying the onset and progression of NAFLD and NASH, and the mechanisms are complexly interacted, and treatments targeting these mechanisms are being investigated[5]. Now the disease concepts of metabolic dysfunction-associated steatotic liver disease (MASLD) and metabolic dysfunction-associated steatohepatitis (MASH) have been proposed and are now being used instead of NAFLD and NASH[6].

Several mouse models of MASH have been reported, including melanocortin-4 receptor (Mc4r) gene deficiency. The Mc4r gene is expressed primarily in the hypothalamus, and knockout mice have been shown to develop cirrhosis after 20 weeks of a high-fat diet and hepatocellular carcinoma by the age of a year; thus, gene knockout (Mc4r-KO) mice are used as a mouse model of MASH[7]. The Mc4r gene contributes to obesity through various mechanisms; it is primarily involved in appetite regulation, therefore Mc4r-KO mice consume more food while using less energy[8].

In this study, we investigated the function of maternal Id-like molecule (Maid) gene, a tumor suppressor gene that was originally discovered as a nuclear-localized protein in mouse maternal transcripts[9]. It interacts with a number of proteins, including cyclin D1 and sirtuin 6, regulates p53 and checkpoint kinase 2 via phosphorylation of ataxia telangiectasia mutated, and plays a role in the regulation of tumorigenesis and inflammation[10]. The role suggested that Maid gene dysfunction could contribute to the onset and progression of MASH.

[1]Division of Gastroenterology and Hepatology, Graduate School of Medical and Dental Sciences, Niigata University, 1-757, Asahimachi-dori, Chuo-ku, Niigata 951-8510, Japan. [2]Department of General Medicine, Niigata University School of Medicine, Niigata University, 1-757, Asahimachi-dori, Chuo-ku, Niigata 951-8510, Japan. ✉email: saka-a@med.niigata-u.ac.jp; terais@med.niigata-u.ac.jp

Therefore, we generated both Maid and Mc4r gene dysfunction mice and compared them with Mc4r-KO mice with high-fat diet, a traditional model of MASH, to evaluate the impact of the Maid gene on the mechanism underlying the development and progression of MAFLD and MASH.

RESULTS

Dysfunction of the Maid gene induced hyperobesity in Mc4r gene-deficient mice

Mice with a Maid gene single knockout did not show obesity at the same level as wild-type, however, mice with a combined Maid and Mc4r gene deletion showed obesity even without a high-fat diet ($p < 0.01$, Fig. 1A, B). In addition, there were no significant differences in dietary intake between Mc4r-KO, Maid-KO; Mc4r-KO, and Mc4r-HFD mice (Fig. 1C).

According to these findings, Maid-KO; Mc4r-KO mice were found to be hyperobese even when not overfed or given a high-fat diet.

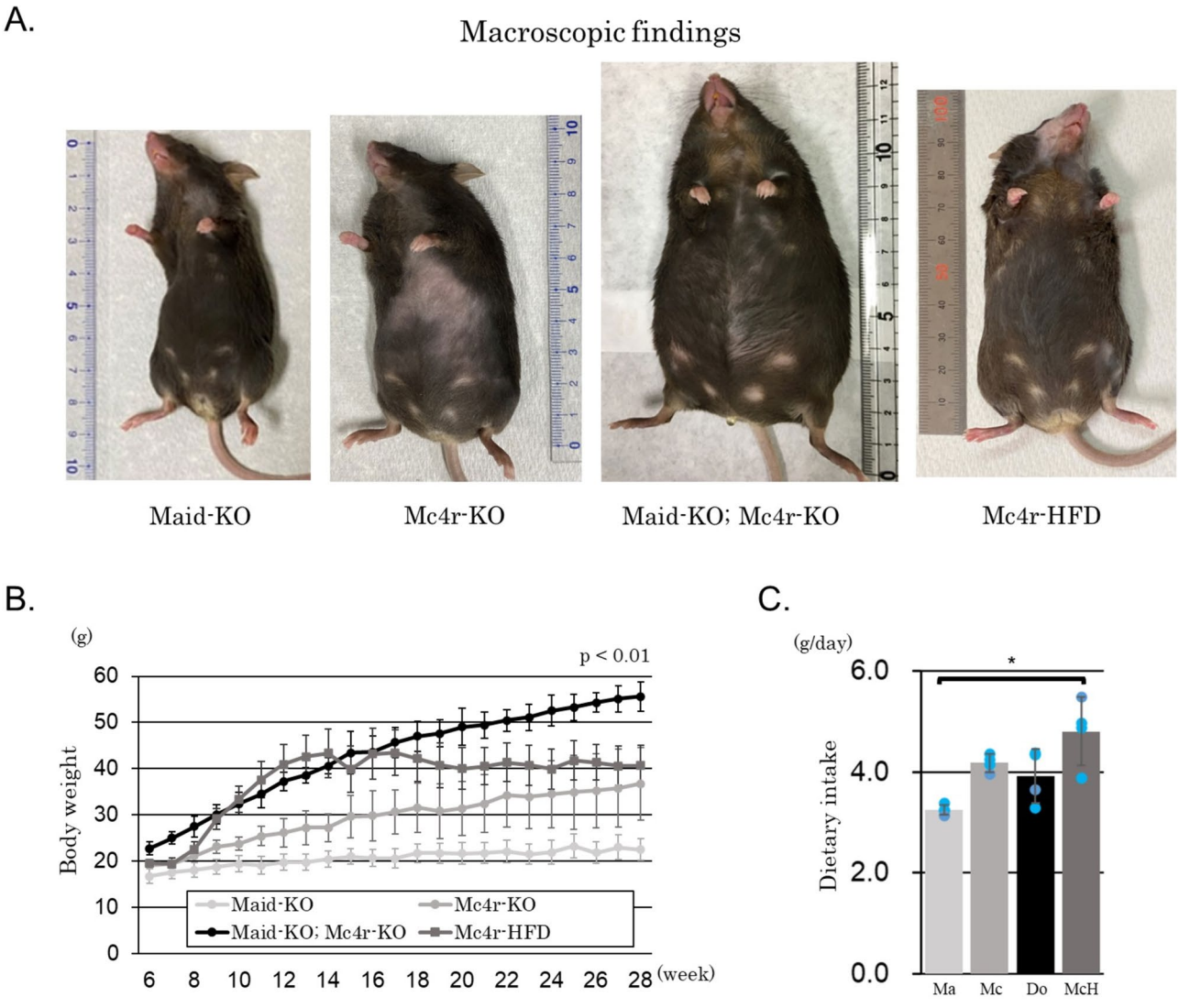

Fig. 1. Dysfunction of Maid gene induced hyperobesity in Mc4r gene deficient mice. Macroscopic findings of Maid-KO, Mc4r-KO, Maid-KO; Mc4r-KO, and Mc4r-HFD female mice at 28 weeks of age (**A**). Changes in body weight over 6–28 weeks of every week in Maid-KO, Mc4r-KO, Maid-KO; Mc4r-KO, and Mc4r-HFD mice and compared by two-way repeated-measures ANOVA with the Tukey–Kramer method [N = 4, (**B**)]. The mean body weight at 28 weeks of age was 22.6 ± 2.3 g in Maid-KO, 36.8 ± 7.9 g in Mc4r-KO, 55.6 ± 3.2 g in Maid-KO; Mc4r-KO mice and 40.7 ± 4.4 g in Mc4r-HFD. Dietary intake compared by one-way ANOVA [3.3 ± 0.1 g/day in Maid-KO, 4.2 ± 0.2 g/day in Mc4r-KO, and 3.9 ± 0.5 g/day in Maid-KO; Mc4r -KO, and 4.8 ± 0.7 g/day in Mc4r-HFD, respectively, N = 4, (**C**)]. *Mc4r* melanocortin 4 receptor, *Mc4r-KO* Mc4r gene knockout, *Maid-KO* maid gene knockout, *Mc4r-HFD* Mc4r-KO mice with high-fat diet, *Ma* maid-KO, *Mc* Mc4r-KO, *Do* maid and Mc4r gene double knockout, *McH* Mc4r-KO mice with high-fat diet. *$p < 0.05$; **$p < 0.01$.

Dysfunction of Maid did not worsen metabolic status or induce liver fibrosis in Mc4r gene-deficient mice

Next, to assess MASLD and related metabolic abnormalities caused by hyperobesity, 28 week-old mice were subjected to liver weight/body weight ratio and liver histological evaluation comparing Maid-KO, Mc4r-KO, Maid-KO; Mc4r-KO, and Mc4r-HFD mice.

Though no significant differences of liver weight/body weight ratio were found in these four groups in female mice (Fig. 2A). Whereas, Maid-KO; Mc4r-KO and Mc4r-HFD mice had significantly higher liver fat deposition than Mc4r-KO mice ($p < 0.01$, Fig. 2B, C). Furthermore, Mc4r-HFD mice had significantly higher liver fibrosis area than Mc4r-KO and Maid-KO; Mc4r-KO mice ($p < 0.01$, Fig. 2B, D).

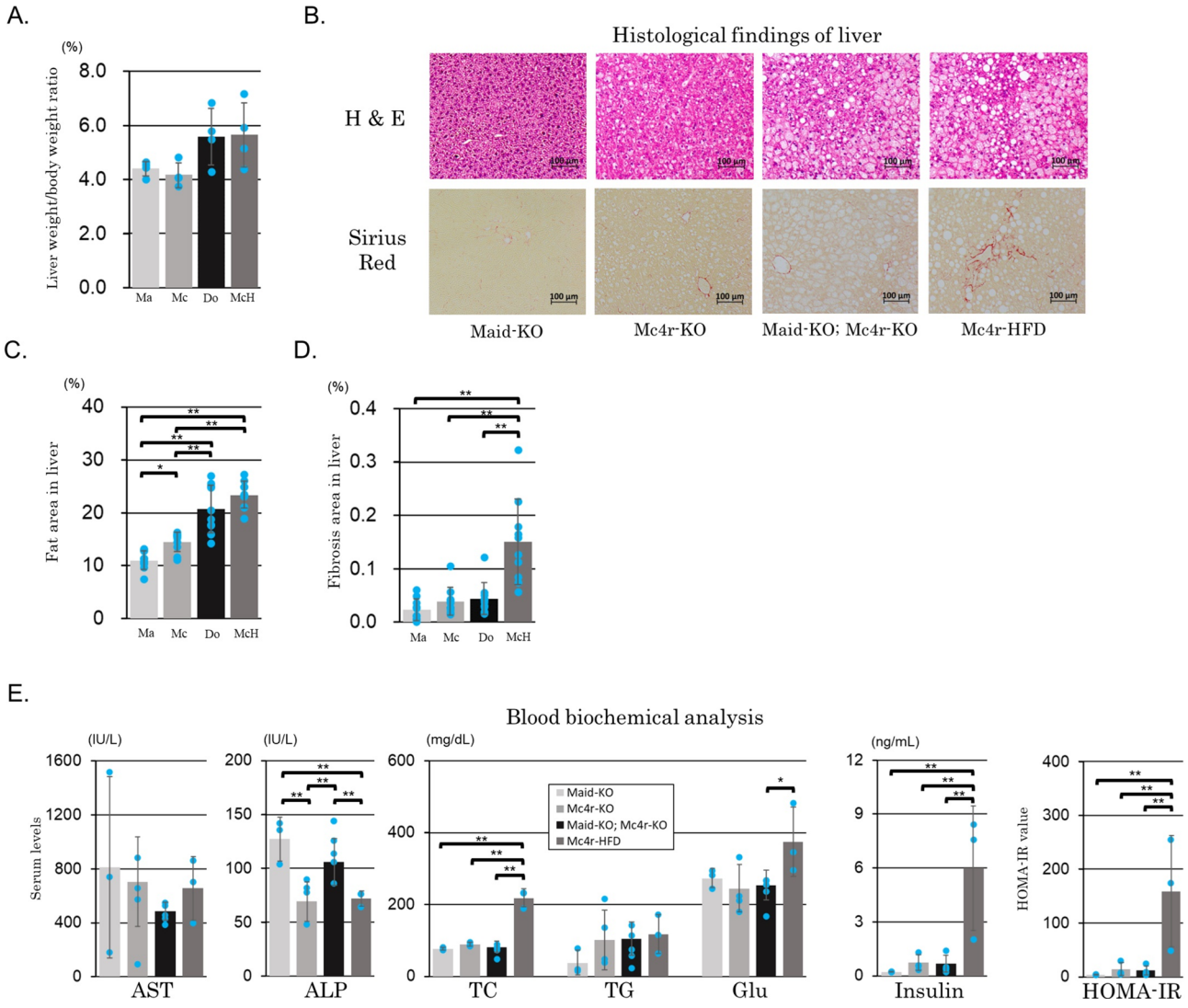

Fig. 2. Dysfunction of the Maid gene did not worsen the metabolic status or induce liver cirrhosis in Mc4r gene-deficient mice. Statistical analysis of the liver weight/body weight ratio at the age of 28 weeks in Maid-KO, Mc4r-KO, Maid-KO; Mc4r-KO and Mc4r-HFD male mice by one-way ANOVA [4.4 ± 0.3% in Maid-KO, 4.2 ± 0.5% in Mc4r-KO, 5.6 ± 1.0% in Maid-KO; Mc4r-KO, and 5.7 ± 1.2% in MC4R-HFD, respectively, N = 4, (**A**)]. Histological findings of the liver by H&E and Sirius red staining of Maid-KO, Mc4r-KO, Maid-KO; Mc4r-KO, and Mc4r-HFD mice at 28 weeks of age (**B**). Statistical analysis of the area of fat deposition [11.0% ± 1.7% in Maid-KO, 14.5% ± 1.9% in Mc4r-KO, 20.7% ± 4.5% in Maid-KO; Mc4r-KO, and 23.4% ± 2.5% in Mc4r-HFD, respectively, (**C**)] and fibrosis [0.02% ± 0.02% in Maid-KO, 0.04% ± 0.03% in Mc4r-KO, 0.04% ± 0.03% in Maid-KO; Mc4r-KO, and 0.15% ± 0.08% in Mc4r-HFD, respectively, (**D**)] in the liver by one-way ANOVA. Blood biochemical analysis of serum aspartate transaminase, alkaline phosphatase, total cholesterol, triglyceride, glucose, insulin levels, and HOMA-IR by one-way ANOVA at the age of 12 weeks (**E**). *Maid-KO* maid gene knockout, *Mc4r-KO* melanocortin 4 receptor gene knockout, *Mc4r-HFD* Mc4r-KO mice with high-fat diet, *H & E*, hematoxylin and eosin, *ANOVA* analysis of variance, *AST* aspartate transaminase, *ALP* alkaline phosphatase, *TC* total cholesterol, *TG* triglyceride, *Glu* glucose, *HOMA-IR* homeostasis model assessment-estimated insulin resistance, *Mc* Mc4r-KO, *Do* maid and Mc4r gene double knockout, *McH* Mc4r-KO mice with high-fat diet. *$p < 0.05$; **$p < 0.01$.

In male mice, there were no significant differences between Maid-KO; Mc4r-KO and Mc4r-HFD mice were found in the change of body weight (Supplemental Fig. 1A) and liver weight/body weight ratio (Supplemental Fig. 1B). Conversely, Mc4r-HFD mice had significantly higher liver fat deposition than Maid-KO; Mc4r-KO and Mc4r-KO mice in males ($p < 0.01$Supplemental Fig. 1C, D). Furthermore, Mc4r-HFD male mice had significantly higher liver fibrosis area than other three groups ($p < 0.01$, Supplemental Fig. 1C, D). These results indicated that female mice are more suitable to assess hyperobesity than male mice because of the significantly higher body weight in Maid-KO; Mc4r-KO than in Mc4r-HFD.

Next, blood biochemical analyses in 12- and 28 week-old mice were performed. It was shown in blood biochemical analysis that Mc4r-HFD mice exhibited hyperlipidemia and hyperinsulinemia compared with Mc4r-KO and Maid-KO; Mc4r-KO in 12 week-old mice ($p < 0.01$, Fig. 2E). Furthermore, the value of homeostasis model assessment-estimated insulin resistance (HOMA-IR), a index of insulin resistance, were also significantly increased in Mc4r-HFD mice than other three groups ($p < 0.01$, Fig. 2E). Otherwise, in 28 week-old mice, Mc4r-HFD showed only hyperlipidemia compared to Mc4r-KO, but there were no significant differences in serum insulin levels and HOMA-IR between four groups ($p < 0.01$, Supplemental Fig. 2).

These results revealed that Maid-KO; Mc4r-KO mice exhibited hyperobesity without liver fibrosis or metabolic abnormalities in contrast to Mc4r-HFD mice.

Maid gene dysfunction reduced the infiltration of macrophages in white adipose tissue

To assess fat accumulation in each adipocyte, the diameter of adipocytes in the visceral white adipose tissue (WAT) of 12 week-old mice was measured. Maid-KO; Mc4r-KO and Mc4r-HFD mice had a significantly larger size of adipocytes than Mc4r-KO mice ($p < 0.01$, Fig. 3A, B). Maid gene dysfunction increased the size of adipocytes as well as their capacity for fat accumulation in each adipocyte, which is similar to high-fat diet.

To investigate tissue inflammation in visceral WAT, cluster of differentiation (CD) 206 and CD11c staining with immunofluorescence was performed. There were no significant differences in the number of CD206-positive cells in the four groups (Fig. 3A, C), while CD11c-positive cells in Maid-KO; Mc4r-KO were significantly fewer than in Mc4r-KO and Mc4r-HFD mice ($p < 0.01$, Fig. 3A, D).

In addition, the expression levels of both inflammatory cytokines (interleukin (IL) -6 and tumor necrosis factor (TNF)-α) and anti-inflammatory cytokines (IL-10 and transforming growth factor (TGF)-β) in Maid-KO; Mc4r-KO were lower than those in Mc4r-KO and Mc4r-HFD ($p < 0.01$ in IL-10, $p < 0.05$ in TNF-α, Fig. 3E) by quantitative PCR.

These findings demonstrated that reducing CD11c-positive cells in Maid-KO; Mc4r-KO mice suppressed adipose tissue inflammation, which contributed to the preservation of large adipocytes while also preventing inflammation from spreading to the liver and promoting liver fibrosis.

Maid gene dysfunction increased fat deposition by adipocytes via sympathetic nerve signaling

Quantitative PCR was used to investigate the cause of increased fat accumulation in adipose tissue, specifically adipocytokines and sympathetic nerve signaling in WAT. Expression levels of adiponectin and resistin in WAT were significantly higher in Maid-KO mice than in other three groups, while expression levels of leptin were significantly higher in Mc4r-HFD mice than in other three groups ($p < 0.05$ in adiponectin and resistin, $p < 0.01$ in leptin, Fig. 3E). This indicated hyperleptinemia and leptin resistance in Mc4r-HFD. Furthermore, the expression of β-3 adrenergic receptor was lower in Maid-KO; Mc4r-KO and Mc4r-HFD mice compared to Mc4r-KO mice without significant difference (Fig. 3E). Therefore, to assess the influence of sympathetic nerve signaling for the fat overaccumulation in visceral fat more exactly, uncoupling protein-1 (UCP1) expression and fat deposition in brown adipose tissue (BAT) were measured. Maid-KO; Mc4r-KO and Mc4r-HFD mice showed significantly higher fat deposition in BAT than in Mc4r-KO mice ($p < 0.01$, Fig. 4A, B). In addition, UCP1 expression in Mc4r-KO mice was significantly higher compared to Maid-KO; Mc4r-KO and Mc4r-HFD mice ($p < 0.01$, Fig. 4A, C).

These results indicated BAT in Maid-KO; Mc4r-KO mice had higher fat deposition and lower expression of UCP1 than those in MC4R-KO mice via sympathetic nerve signaling and β-3 adrenergic receptor.

Discussion

Following hypertrophy of the adipocytes, inflammation, and macrophage infiltration into adipose tissue resulted in the production of several chemokines[11]. Anti-inflammatory M2 macrophages are present in healthy adipose tissue and contribute to maintaining the tissue's homeostasis[12], whereas in adipose tissue with excessive fat accumulation, inflammatory M1 macrophages increase and macrophages become M1-dominant[13].

Chronic inflammation in adipose tissue caused by M1 macrophages impairs adipose tissue function and disrupts the production of adipocytokines, therefore inflammatory cytokines like TNF-α and IL-6 increase while anti-inflammatory cytokines like adiponectin decrease. This dysregulation of adipocytokines leads to insulin resistance throughout the body. Furthermore, the function of fat and energy accumulation also gets impaired, leading to ectopic fat accumulation in organs such as the liver[14]. Furthermore, removing M2 macrophages reduced TGF-β expression, leading to healthy conditions in adipocytes[15,16]. While CD11c is known as a marker of dendritic cells, it is also reported as a marker of M1 macrophages[15,16]. In the current study, the number of CD11c-positive cells in adipose tissue was reduced in Maid-KO; Mc4r-KO mice, and quantitative PCR revealed a decrease in inflammatory and anti-inflammatory cytokines, indicating that adipose tissue-induced inflammation was reduced.

Leptin is an adipocytokine secreted primarily by adipocytes it acts on the central nervous system via the bloodstream to suppress food appetite and increase energy expenditure by activating the sympathetic nervous system. Leptin production increases with fat accumulation in adipocytes, contributing to maintain long-term homeostasis of energy metabolism[17]. Leptin is located upstream of melanocortin in the hypothalamus, so deleting

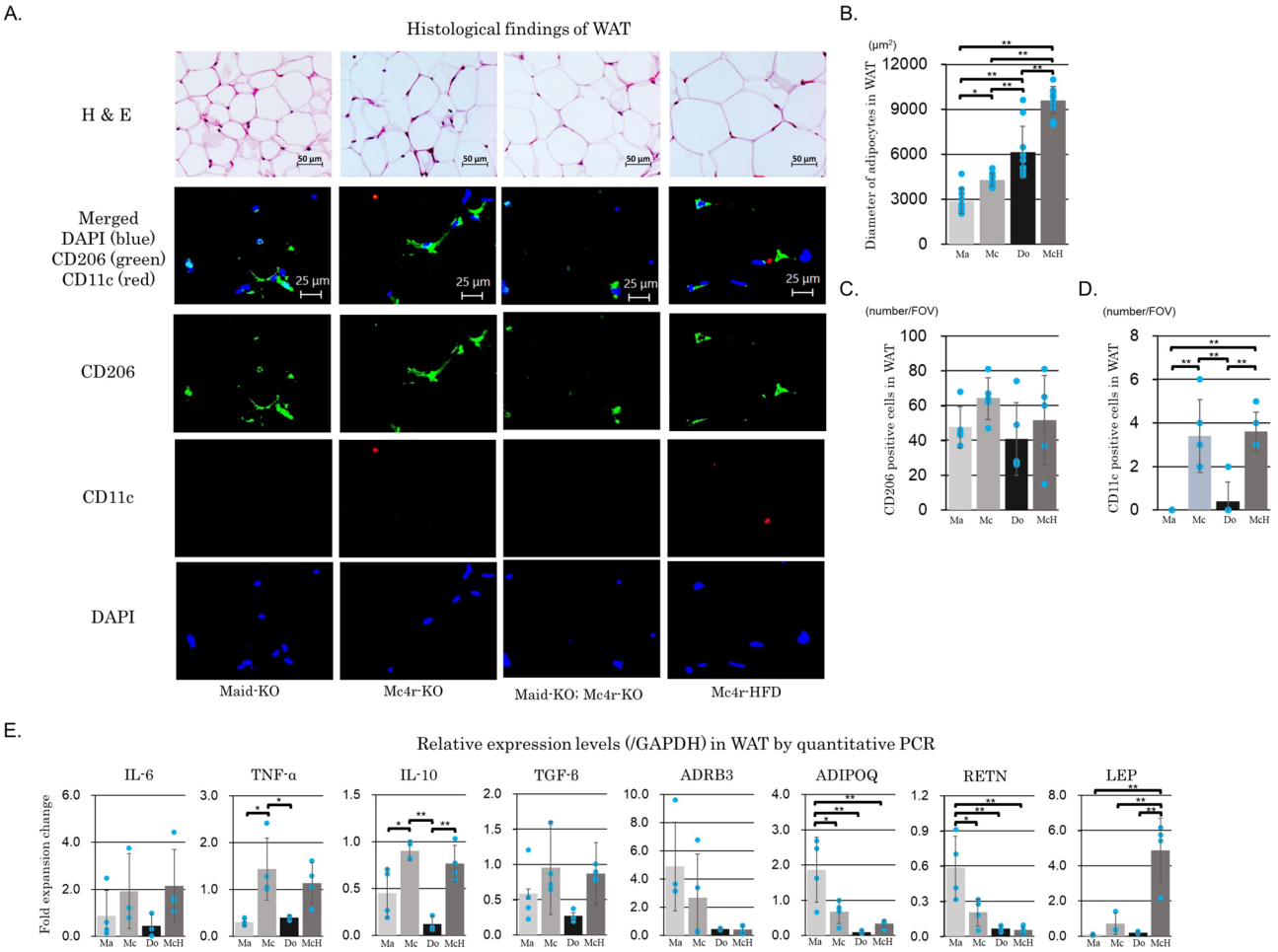

Fig. 3. Maid gene dysfunction reduced the infiltration of macrophages in white adipose tissue. Histological findings of WAT by H & E staining and immunofluorescence by CD206 and CD11c double labeling of Maid-KO, Mc4r-KO, Maid-KO; Mc4r-KO, and Mc4r-HFD mice at 12 weeks of age [N = 4, (**A**), green, CD206 marking; red, CD11c marking; and blue, DAPI]. Statistical analysis by one-way ANOVA of the diameter of adipocytes [2890 ± 830 μm^2 in Mc4r -KO, 4290 ± 430 μm2 in Mc4r -KO, 6140 ± 1730 μm2 in Maid-KO; Mc4r-KO, and 9600 ± 930 μm^2 in Mc4r-HFD, respectively, (**B**)] and the cell number of CD206-positive [47.6 ± 11.9 cells/FOV in Maid-KO, 64.2 ± 12.2 cells/FOV in Mc4r-KO, 40.8 ± 20.9 cells/FOV in Maid-KO; Mc4r-KO, and 51.6 ± 25.8 cells/FOV in Mc4r-HFD, respectively, (**C**)] and CD11c-positive [0.0 ± 0.0 cells/FOV in Maid-KO, 3.4 ± 1.7 cells/FOV in Mc4r-KO, 0.4 ± 0.9 cells/FOV in Maid-KO; Mc4r-KO, and 3.6 ± 0.9 cells/FOV in Mc4r-HFD, respectively, (**D**)]. The quantitative PCR of mRNA extracted in WAT in Maid-KO, Mc4r-KO, Maid-KO; Mc4r-KO, and Mc4r-HFD mice at the age of 12 weeks (**E**). *WAT* white adipose tissue, *H & E* hematoxylin and eosin, *CD* cluster of differentiation, *DAPI* 4′,6-diamidino-2-phenylindole, *Mc4r-KO* melanocortin 4 receptor gene knockout, *Maid-KO* maid gene knockout, *Mc4r-HFD* Mc4r-KO mice with high-fat diet, *ANOVA* analysis of variance, *FOV* field of view, *IL* interleukin, *TNF* tumor necrosis factor, *TGF* transforming growth factor, *ADRB3* adrenergic receptor β-3, *ADIPOQ* adiponectin, *RETN* resistin, *LEP* leptin, *Ma* maid-KO, *Mc* Mc4r-KO, *Do* maid and MC4R gene double knockout McH, *Mc4r-KO* mice with high-fat diet, *GAPDH* glyceraldehyde-3-phosphate dehydrogenase. *p < 0.05, **p < 0.01.

the Mc4r gene results in a leptin-insensitive state in some hypothalamic leptin signaling pathways[18]. Furthermore, Mc4r is associated with the function of adipose tissue via the sympathetic nervous system, and Mc4r gene dysfunction contributes to fat overaccumulation in WAT and BAT[19]. BAT is a specialized adipose tissue with the ability to produce heat. Brown adipocytes contain numerous mitochondria and UCP1, a heat-producing protein, is localized in the inner mitochondrial membrane. Heat production in BAT is regulated by the sympathetic nervous system, and heat is produced by the action of UCP1 when noradrenaline released from sympathetic nerve endings is received by brown adipocytes through β3 adrenergic receptors[20]. In addition, β3 adrenergic receptors are also expressed in WAT, and sympathetic stimulation promotes lipolysis in adipocytes[21]. There had been lower levels of UCP1 expression, and more fat deposition in WAT and BAT in Maid-KO; Mc4r-KO mice than in Mc4r-KO mice. This suggests that inhibition of sympathetic signaling pathways was more severe in Maid-KO; Mc4r-KO mice than in Mc4r-KO mice, leading to hyperobesity.

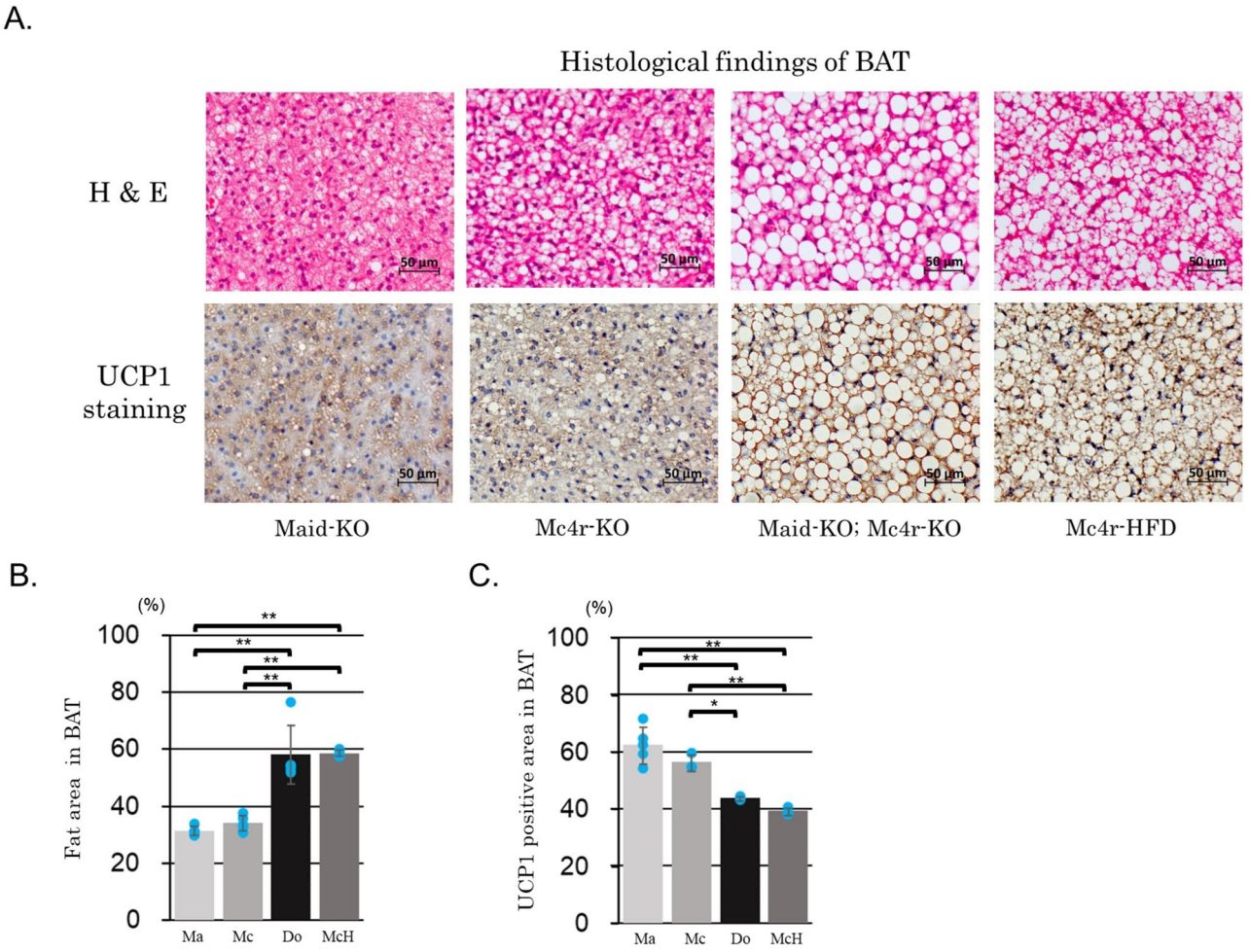

Fig. 4. Maid gene dysfunction increased the fat deposition of adipocytes via sympathetic nerve signaling. Histological findings of BAT by H&E staining and immunohistochemistry by UCP1 in Maid-KO, Mc4r-KO, Maid-KO; Mc4r-KO, and Mc4r-HFD mice at 12 weeks of age [N = 4, (**A**)]. Statistical analysis of fat deposition area [31.4% ± 1.5% in Maid-KO, 34.1% ± 2.6% in Mc4r-KO, 58.1% ± 10.4% in Maid-KO; Mc4r-KO, and 58.6% ± 1.2% in Mc4r-HFD, respectively, $p < 0.01$, (**B**)] and UCP1 positive area [62.4% ± 6.4% in Maid-KO, 56.3% ± 2.9% in Mc4r-KO, 43.6 ± 0.8% in Maid-KO; Mc4r-KO, and 39.2% ± 1.2% in Mc4r-HFD, respectively, (**C**)] in BAT by one-way ANOVA. *BAT* brown adipose tissue, *UCP1* uncoupling protein-1, *Mc4r-KO* melanocortin 4 receptor gene knockout, *Maid-KO* maid gene knockout, *Mc4r-HFD* Mc4r-KO mice with high-fat diet, *ANOVA* analysis of variance, *Ma* Maid-KO, *Mc* MC4R-KO, *Do* maid and Mc4r gene double knockout, *McH* Mc4r-KO mice with high-fat diet. *$p < 0.05$; **$p < 0.01$.

Hyperinsulinemia and hyperleptinemia are frequently observed in human patients with steatohepatitis, and promote liver inflammation and fibrosis in animal MASH models[22,23]. At 12 weeks, Mc4r-HFD mice have higher serum insulin levels and WAT leptin expression than Mc4r-KO and Maid-KO; Mc4r-KO mice, and liver fibrosis were observed in Mc4r-HFD mice by the result of the high insulin and leptin levels.

This study has a limitation. Although the Maid gene is expressed in multiple organs throughout the body[9], we were unable to determine which organ is required for Maid gene deletion using organ-specific conditional knockout mice.

In conclusion, Maid gene deficiency in Mc4r-KO mice causes a hyperobese phenotype through two mechanisms: the inhibition of sympathetic signaling pathways and reduction of macrophages and adipocytokines in adipose tissue, but not steatohepatitis and fibrosis. Maid and MC4R gene-deficient mice may be useful as a new model of MASLD with hyperobesity and less systemic inflammation and metabolic problems for studying the mechanism of MASH progression when compared to the mouse model with high-fat diet.

Methods

Animals

Mc4r-KO mice with a C57BL/6J background that generated protocol was reported by Balthasar N, et al.[24]. Mc4r gene dysfunction is induced by the insertion of a loxP-flanked transcriptional blocking sequence between the transcription start site and the ATG of the Mc4r gene. The Mc4r-KO mice kindly provided by Dr. Takayoshi Suganami (Nagoya University) and Dr. Yoshihiro Ogawa (Kyushu University) and Maid gene knockout (Maid-KO) mice with a C57BL/6J background that generated protocol was reported by Sonnenberg-Riethmacher E,

et al.[10]. Maid gene dysfunction is induced by the deletion of exon 4. The Maid-KO mice kindly provided by Yamaguchi University were used.

Maid-KO; Mc4r-KO mice were created by crossing Maid-KO and Mc4r-KO mice in our facility and cross-bred each three genotypes: Mc4r-KO, Maid-KO, and Maid-KO; Mc4r-KO mice. Four randomly selected mice were housed in individual cages with controlled environmental settings (temperature of 20–23 °C, humidity of 45%–55%, 12-h dark/light cycles). The mice had unrestricted access to food and water in areas that were designated as pathogen-free. All animal experiments were done following the guidelines reviewed by the Institutional Animal Care and Use Committee of Niigata University. This study was approved by the President of Niigata University (approval number: SA01130). The study was carried out in compliance with the ARRIVE guidelines 2.0.

Development of animal models

Eight female mice were examined for each genotype: wild-type, Maid-KO, Mc4r-KO, and Maid-KO; Mc4r-KO. All mice were fed CE-2 (CLEA Japan, Inc., Tokyo, Japan), the standard diet for mice. Additionally, another eight Mc4r-KO female mice were fed a high-fat diet (Western Diet D12079BM, Research Diets, Inc., New Brunswick, NJ, USA) from the age of 8 to 28 weeks. The amount of dietary intake was calculated from the weight decrease in measurements of food boxes twice a week. Half of the mice (n = 4) were sacrificed at 12 weeks, and the other half were sacrificed at 28 weeks. The mice were sacrificed by cervical dislocation under isoflurane anesthesia 2–4 h after fasting, and the blood sample was collected from the heart immediately. Liver tissues, WAT from the intraperitoneum, and BAT from the intrascapular region were removed, and some of the samples were stored in 10% formalin solution. The residual WAT was promptly frozen using liquid nitrogen and stored at − 80 °C.

Histological analysis

Liver and adipose tissue samples were fixed in 10% formalin before being paraffin-embedded. Hematoxylin and eosin staining, Sirius red staining, immunohistochemistry, and immunofluorescence were then performed. Immunohistochemistry was performed using UCP1 antibody (GTX112784; GeneTex, Inc., CA, USA) at 1:500 dilution along with Vectastain Elite ABC rabbit IgG kit (PK-6101; Vector Laboratories, CA, USA) and DAB chromogen tablets (Muto Pure Chemicals, Tokyo, Japan). The immunofluorescence process was performed using CD206 antibody (ab64693, Abcam, Cambridge, United Kingdom) at 1:500 and CD11c antibody (ab33483, Abcam, Cambridge, United Kingdom) at 1:100 dilution, with Donkey anti-Rabbit IgG, Alexa Fluor™ 488 (A-21206; Invitrogen, CA, USA), goat anti-American Hamster, Alexa Fluor™ 568 (A-78965; Invitrogen, CA, USA), and VECTASHIELD® Antifade Mounting Medium with 4′,6-diamidino-2-phenylindole (H-1200, Vector laboratories, CA, USA).

Images were taken randomly for each tissue section and quantitatively assessed using ImageJ software (version 1.8.0_172; National Institutes of Health, Bethesda, MD, USA) with an RGB-based protocol, as reported previously[25]. The diameter of adipocytes was measured the largest adipocyte in randomly taken images.

Blood chemistry and cholesterol concentrations

Serum levels of aspartate transaminase, alkaline phosphatase, total cholesterol, triglycerides, and glucose were measured by Oriental Yeast Co., Ltd. Nagahama LSL (Nagahama, Japan). Serum samples were employed in an insulin enzyme-linked immunosorbent assay kit (M1104; Morinaga Institute of Biological Science, Inc., Yokohama, Japan) following the manufacturer's instructions. HOMA-IR was calculated as previously reported method[26].

Quantitative PCR in the WAT

Total RNA was extracted from WAT using an RNeasy Lipid Tissue Mini kit (Qiagen, Hilden, Germany), which was then reverse-transcribed into cDNA using a qScript™ cDNA SuperMix (Quantabio, Beverly, MA, USA). Gene expression was measured using quantitative PCR with a real-time PCR primer set for adipose tissue (PCRM2, Cosmo Bio Co., LTD, Tokyo, Japan), SYBR Green, and the StepOnePlus System (Thermo Fisher Scientific, Waltham, MA, USA). The real-time PCR was performed as follows: 95 °C for 10 min followed by 50 cycles of 95 °C for 15 S and 60 °C for 1 min. Reactions were incubated at 95 °C for 15 S, 60 °C for 1 min, and 95 °C for 15 S for final dissociation, at the completion of the cycling. The results were analyzed with the bundled software. Moreover, changes in gene expression were measured using the $2^{-\Delta\Delta Ct}$ method, with gene expression normalized to that of glyceraldehyde-3-phosphate dehydrogenase (GAPDH) in each sample.

Statistical analysis

The data is presented as means ± standard deviation. The groups were compared using one-way analysis of variance (ANOVA) or two-way repeated-measures ANOVA with the Tukey–Kramer method. The threshold for statistical significance was set at $P < 0.05$. The calculations were performed using GraphPad Prism Version 6.0 (GraphPad Software, Inc., Boston, MA, USA).

Data availability

The datasets analyzed during the current study available from the corresponding author on reasonable request.

Received: 17 April 2024; Accepted: 4 September 2024
Published online: 10 September 2024

References

1. Enomoto, H. *et al.* Transition in the etiology of liver cirrhosis in Japan: A nationwide survey. *J. Gastroenterol.* **55**, 353–362 (2020).
2. Enomoto, H. *et al.* The transition in the etiologies of hepatocellular carcinoma-complicated liver cirrhosis in a nationwide survey of Japan. *J. Gastroenterol.* **56**, 158–167 (2021).
3. Younossi, Z. M. *et al.* Global epidemiology of nonalcoholic fatty liver disease-Meta-analytic assessment of prevalence, incidence, and outcomes. *Hepatology* **64**, 73–84 (2016).
4. Estes, C. *et al.* Modeling NAFLD disease burden in China, France, Germany, Italy, Japan, Spain, United Kingdom, and United States for the period 2016–2030. *J. Hepatol.* **69**, 896–904 (2018).
5. Perazzo, H. & Dufour, J. F. The therapeutic landscape of non-alcoholic steatohepatitis. *Liver Int.* **37**, 634–647 (2017).
6. Rinella, M. E. *et al.* A multisociety Delphi consensus statement on new fatty liver disease nomenclature. *Ann. Hepatol.* **29**, 101133 (2024).
7. Itoh, M. *et al.* Melanocortin 4 receptor-deficient mice as a novel mouse model of nonalcoholic steatohepatitis. *Am. J. Pathol.* **179**, 2454–2463 (2011).
8. Schwartz, M. W., Woods, S. C., Porte, D., Seeley, R. J. & Baskin, D. G. Central nervous system control of food intake. *Nature* **404**, 661–671 (2000).
9. Terai, S., Aoki, H., Ashida, K. & Thorgeirsson, S. S. Human homologue of maid: A dominant inhibitory helix-loop-helix protein associated with liver-specific gene expression. *Hepatology* **32**, 357–366 (2000).
10. Sonnenberg-Riethmacher, E., Wüstefeld, T., Miehe, M., Trautwein, C. & Riethmacher, D. Maid (GCIP) is involved in cell cycle control of hepatocytes. *Hepatology* **45**, 404–411 (2007).
11. Weisberg, S. P. *et al.* Obesity is associated with macrophage accumulation in adipose tissue. *J. Clin. Investig.* **112**, 1796–1808 (2003).
12. Toda, G. *et al.* Insulin- and lipopolysaccharide-mediated signaling in adipose tissue macrophages regulates postprandial glycemia through Akt-mTOR activation. *Mol. Cell* **79**, 43–53 (2020).
13. Lumeng, C. N., Bodzin, J. L. & Saltiel, A. R. Obesity induces a phenotypic switch in adipose tissue macrophage polarization. *J. Clin. Investig.* **117**, 175–184 (2007).
14. Suganami, T. & Ogawa, Y. Adipose tissue macrophages: Their role in adipose tissue remodeling. *J. Leukoc. Biol.* **88**, 33–39 (2010).
15. Nawaz, A. *et al.* CD206(+) M2-like macrophages regulate systemic glucose metabolism by inhibiting proliferation of adipocyte progenitors. *Nat. Commun.* **8**, 286 (2017).
16. Nawaz, A., Fujisaka, S., Kado, T., Jeelani, I. & Tobe, K. Heterogeneity of adipose tissue-resident macrophages-beyond M1/M2 paradigm. *Diabetol. Int.* **14**, 125–133 (2023).
17. Martelli, D. & Brooks, V. L. Leptin increases: Physiological roles in the control of sympathetic nerve activity, energy balance, and the hypothalamic-pituitary-thyroid axis. *Int. J. Mol. Sci.* **24**, 2684 (2023).
18. Balthasar, N. Genetic dissection of neuronal pathways controlling energy homeostasis. *Obesity* **14**, 222s–227s (2006).
19. Morgan, D. A. *et al.* Regulation of glucose tolerance and sympathetic activity by MC4R signaling in the lateral hypothalamus. *Diabetes* **64**, 1976–1987 (2015).
20. Cannon, B. & Nedergaard, J. Brown adipose tissue: Function and physiological significance. *Physiol. Rev.* **84**, 277–359 (2004).
21. Yang, S. *et al.* The role of β3-adrenergic receptors in cold-induced beige adipocyte production in pigs. *Cells* **13**, 709 (2024).
22. Honda, H. *et al.* Leptin is required for fibrogenic responses induced by thioacetamide in the murine liver. *Hepatology* **36**, 12–21 (2002).
23. Longo, M. *et al.* Adipose tissue dysfunction as determinant of obesity-associated metabolic complications. *Int. J. Mol. Sci.* **20**, 2358 (2019).
24. Balthasar, N. *et al.* Divergence of melanocortin pathways in the control of food intake and energy expenditure. *Cell* **123**, 493–505 (2005).
25. Vrekoussis, T. *et al.* Image analysis of breast cancer immunohistochemistry-stained sections using ImageJ: An RGB-based model. *Anticancer Res.* **29**, 4995–4998 (2009).
26. Matthews, D. R. *et al.* Homeostasis model assessment: Insulin resistance and beta-cell function from fasting plasma glucose and insulin concentrations in man. *Diabetologia* **28**, 412–419 (1985).

Author contributions

AS, KeK, and ST designed the study. KyK, AS, SM, IN, MK, and YT generated, collected, analyzed, and interpreted the data. NK, YA, HA, and KeK analyzed and interpreted the metabolic profile. KyK and AS prepared the manuscript. ST participated in the review of the manuscript and final approval. All authors thoroughly reviewed the manuscript. All authors read and approved the final version of this manuscript.

Funding

This study was supported in part by a Grant-in-Aid for Scientific Research (22K08006 and 22H03055) from the Japan Society for the Promotion of Science.

Competing interests

The authors declare no competing interests.

Additional information

Supplementary Information The online version contains supplementary material available at https://doi.org/10.1038/s41598-024-72217-1.

Correspondence and requests for materials should be addressed to A.S. or S.T.